Supporting Information

Type-II Core/Shell Si/CdS Nanocrystals: Synthesis, Spectroscopic and Electrical Properties

Guan Wang,[‡a] Jianwei Ji,[‡a] Chengdong Li,[b] Linwei Yu,[b] Weikuan Duan,[c] Wei Wei,[c] Xiaozeng You*[a] and Xiangxing Xu*[a]

[a] *State Key Laboratory of Coordination Chemistry, School of Chemistry and Chemical Engineering, Nanjing National Laboratory of Microstructures, Nanjing University, Nanjing 210093, P. R. China.*
[b] *School of Electronics Science and Engineering, National Laboratory of Solid State Microstructures, Nanjing University, 210093, Nanjing, China,*
[c] *School of Optoelectronic Engineering, Nanjing University of Posts and Telecommunications, Nanjing 210023, P. R. China.*
‡ G. Wang and J. W. Ji contribute equally.
* correspond to: xuxx@nju.edu.cn; youxz@nju.edu.cn

Experimental Section

Chemicals. $HSiCl_3$ (99%), decane (99%), oleylamine (OY, 80%-90%), 1-decene (95%), 3-Mercaptopropionic acid (MPA, 98%) and cadmium oxide (CdO, 99%) were purchased from Aladdin Reagent (China) Co., Ltd. 1-octadecene (ODE, 90%) and oleic acid (OA, 90%) were obtained from Alfa Aesar. Analytical grade sulfur (S, 5N), ethanol (99.5%), cyclohexane (99.5%) and hydrofluoric acid (40% aqueous solution) were received from Sinopharm Chemical Reagent Co., Ltd. (SCRC). All reagents were used as purchased without further purification.

Instruments. The X-ray powder diffraction (XRD) spectrum was performed on a Bruker D8 Advance instrument with a Cu Kα radiation (λ = 1.5418 Å). high resolution transmission electron microscopy (HRTEM) images and energy dispersive X-ray spectroscopy (EDS) were obtained on a JEM–2100 transmission electron microscopy with the acceleration voltage of 200 kV. Scanning transmission electron microscopy (STEM) images were measured on FEI Tecnai G2 F20 with the acceleration voltage of 200KV. The X-ray photoelectron spectroscopy (XPS) data were recorded by PHI 5000 VersaProbe (U1VAC-PHI). The photoluminescence (PL) spectra were collected by a Hitachi F–4600 fluorescence spectrophotometer. The UV-vis absorption spectra were measured by a Shimadzu UV-2700 UV-vis spectrophotometer. Electronic semiconducting property was recorded a semiconductor device analyzer B1500A from Agilent Technologies. The PL lifetime was obtained on a Zolix Omini-λ 300 fluorescence spectrophotometer.

Synthesis of hydrogen terminated freestanding Si QDs. A hydrogen reduction method were employed to synthesis QDs. Typically, 5 mL $HSiCl_3$ (6.7 g, 49.5 mmol) was added to a three-necked flask with a magnetic stir bar and kept at –78°C for 10 min, using standard Schlenk techniques with N_2 protection. When the temperature of liquid cooled down, 20 mL (~1.1 mmol) distilled water was injected with stirring. A large quantity of white precipitate and HCl (g) were formed immediately. The precipitate was collected by centrifugation, washed by distilled water and dried under vacuum at 60 °C overnight. This white powder $(HSiO_{1.5})_n$ was used for further reaction. The $(HSiO_{1.5})_n$ powder (1.10 g, 25 mmol) was placed in a corundum crucible and transferred to a tube furnace at room temperature. Then the temperature was ramped to 1150 °C at the speed of 5 °C/min and maintained for 1 hrs under a slightly reducing atmosphere containing 5% H_2 and 95% Ar (≥99.999%). Light brown product of Si/SiO_2 composite was collected when cooled to room temperature,. The composite was grinded by a mortar and pestle for 10 min. The grinded composite (0.10 g) were transferred to a Teflon container (20 mL) with a magnetic stir bar. A mixture of ethanol (3 mL) and hydrofluoric acid (40%, 5 mL) were added. The light brown mixture was stirred for 60 min to allow the dissolve of the SiO_2. Finally, 10 mL decane (99%) and 15 mL 1-decene were added to extract the hydrogen terminated Si QDs into the upper organic phase, forming a cloudy light brown suspension, which was isolated and saved for further surface modification.

Modification of Si QDs by 1-decene. The as prepared suspension (12 mL) of Si QDs was loaded in a 50 mL three-neck-flask equipped with a reflux condenser. Then the solution was degassed by a vacuum pump for 10 min. Protected by nitrogen, the solution was heated to 156 °C and kept for 8 hours. Cooling down to room temperature, the resulting transparent orange solution was centrifuged for 15 min at 2000 rpm. The transparent orange supernatant was collected leaving some brown solid of Si QDs of limited dispersibility. The solvent and excess ligand was removed by vacuum distillation, leaving a reddish brown solid product. These decyl-modified Si QDs were well-redispersed in 10 mL nonpolar solvent (in ODE for CdS shell growth and in cyclohexane for spectroscopic characterization) to give a transparent orange solution.

Preparation of cadmium oleic acid (CdOA), sulfur ODE solution (S-ODE) and CdS QDs. *CdOA solution* (0.07 mol/L): CdO (0.068 g, 0.5 mmol) was mixed with OA (2.2 ml) and ODE (5 ml) in a 50 ml three neck flask. The mixture was heated to 250 °C under nitrogen protection until the brown solution turned colorless. *S-ODE solution* (0.07 mol/L): The sulfur precursor was prepared by dissolving sulfur (0.011 g, 0.35 mmol) in ODE (5 mL) at 80 °C under nitrogen protection. *CdS QDs*: 3

mL OY was mixed with 10 mL ODE, 0.2 mL S-ODE and 0.2 mL CdOA in a 50 ml three neck flask. The mixture was heated to 200 °C under nitrogen protection and kept for 10 min. Cooled to room temperature, the CdS QDs were precipitated by adding ethanol and centrifugation (14000 rpm, 5 min). The collected QDs were then redispersed in cyclohexane, washed with ethanol and centrifugation for a second time. The final CdS QDs were well dispersed and stored in cyclohexane.

The growth of CdS shell on Si QDs. The Si QDs ODE solution (10 mL) was loaded in a 50 mL three-neck-flask equipped with a reflux condenser. It was degassed by a vacuum pump for 10 min. Protected by nitrogen, 50 μL S-ODE solution was injected in through a syringe and then the temperature was raised to 180 °C for 10 min; then 3 mL OM and 50 μL CdOA solution were injected in to grow the CdS shell for another 10 min. This shell growth step was repeated for required times to get Si/CdS NCs of different shell thickness. The amount of the S-ODE and CdOA precursors for each growth round is listed in Table S1. For the final step, the temperature was raised to 200 °C and kept for 10 min to complete the shell growth. Naturally cooling to room temperature, The Si/CdS NCs were collected by adding ethanol and centrifugation (14000 rpm, 15 min). It was redispersed in cyclohexane, washed with ethanol and centrifuged for a second time. These Si/CdS NCs were well dispersed and stored in cyclohexane.

Table S1. List of the SILAR growth parameters for Si/CdS-1 and Si/CdS-2 samples.

Growth / Sample		1st	2nd	3rd	4th	5th	6th	7th
Si/CdS-1	S-ODE 10 min	50 μL	50 μL	0.1 mL	0.1 mL			
	CdOA 10 min	50 μL	50 μL	0.1 mL	0.1 mL			
Si/CdS-2	S-ODE 10 min	50 μL	50 μL	0.1 mL	0.1 mL	0.1 mL	0.1 mL	0.1 mL
	S-ODE 10 min	50 μL	50 μL	0.1 mL	0.1 mL	0.1 mL	0.1 mL	0.1 mL

Sample preparation for current-voltage (I-V) measurement. Since surface ligands (oleate and/or oleylamine) with long alkyl chains behave as dielectric tunneling barriers hindering the charge transfer between neighboring NCs, small molecules of mercaptopropionic acid (MPA) was adopted to exchange with the ligands to make a closer distance of neighboring Si/CdS or CdS NCs. Solution A was prepared by mixing MPA (0.17 mL), H_2O (0.3 mL) and CH_3OH (1 mL) with the pH adjusted to 8-9 by using NaOH aqueous solution. It was added to the $CHCl_3$ solution (5 mL) of CdS or Si/CdS

nanocrystals. After stirring 30 min, 10 mL H_2O was added and kept stirring for another 20 min. The aqueous phase was separated. The MPA exchanged/modified nanocrystals were collected by adding acetone to the aqueous phase and centrifugation (4000 rpm, 20 min). All the samples were dried in vacuum at 60 ℃ overnight. The powder was collected and pressed into a pellet with a diameter of 6 mm and thickness of ~ 1 mm under 3 MPa. Aluminum electrodes were fabricated on the pellet by thermal evaporation-deposition with a gap of 2 mm for the following current-voltage (I-V) measurement.

Figures:

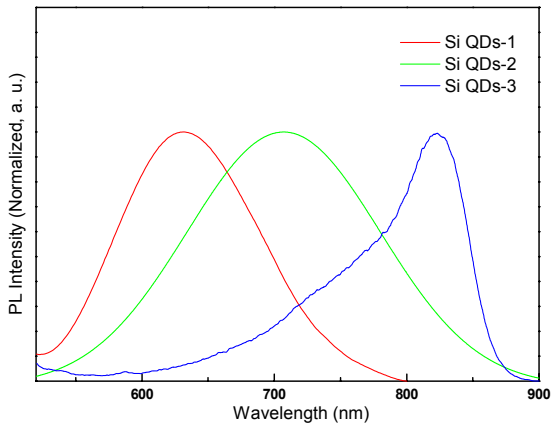

Fig. S1 PL spectra of Si QDs of increasing average size from Si QDs-1 (~2.5 nm), Si QDs-2 (~3.5 nm) to Si QDs-3 (~5.4 nm). It was controlled by the H_2 reduction time of Si QDs-1: 1hr; Si QDs-2: 1.5 hr; Si QDs-3: 2hr. Excitation: 360 nm for Si QDs-1, 500 nm for Si QDs-2 and Si QDs-3. Si QDs-1 was used in this manuscript.

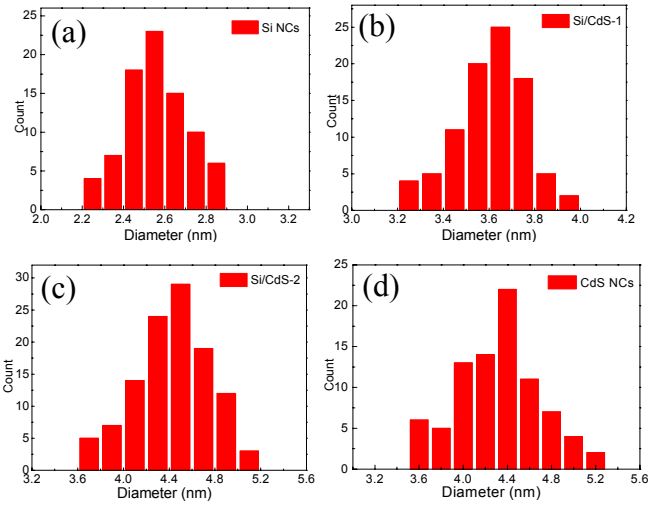

Fig. S2 Size distributions of Si, Si/CdS-1, Si/CdS-2 and CdS NCs measured from HRTEM images.

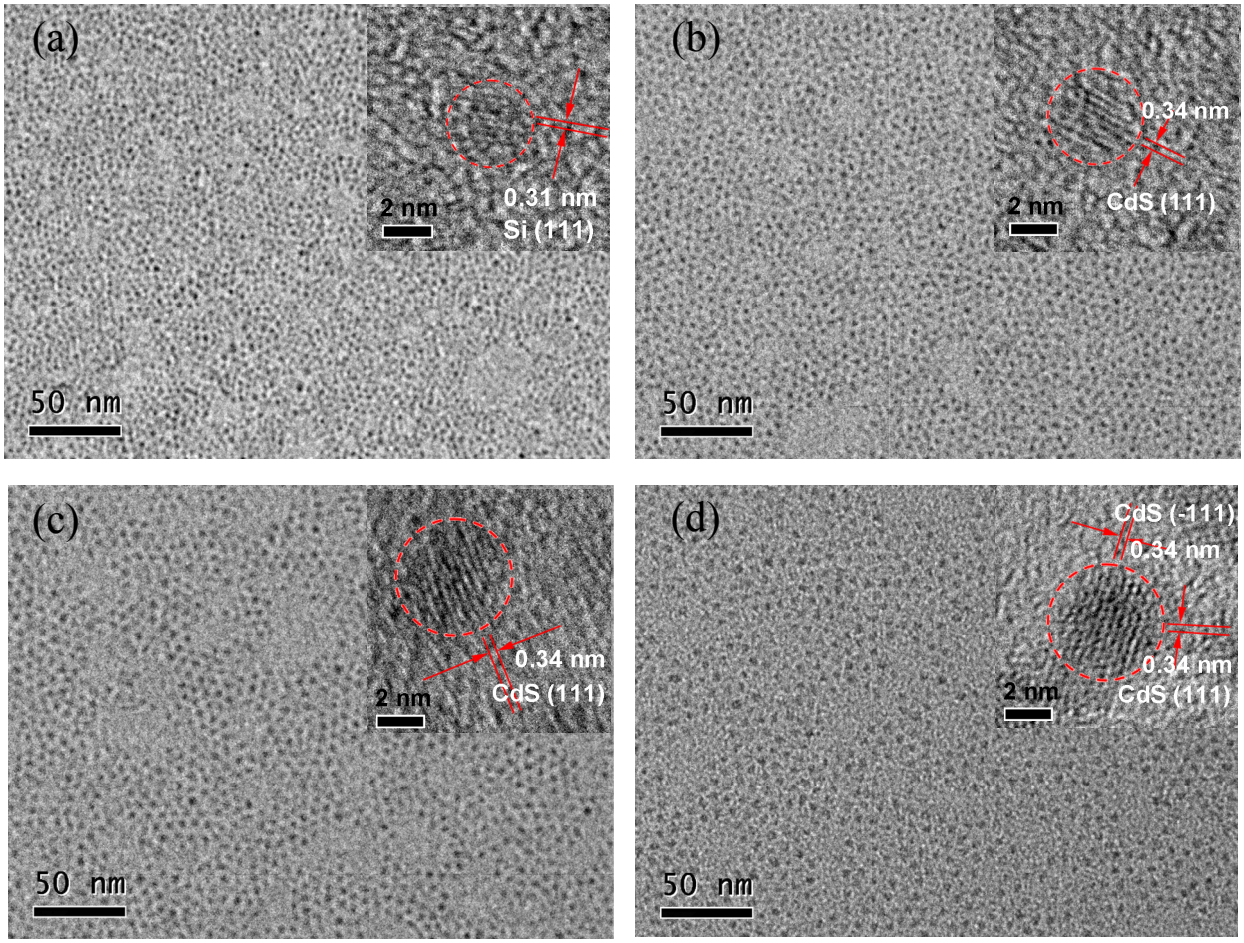

Fig. S3 Magnified TEM/HRTEM images in Fig 1 in the manuscript. (a) Si QDs, (b) Si/CdS-1 NCs (c) Si/CdS-2 NCs and (d) CdS NCs.

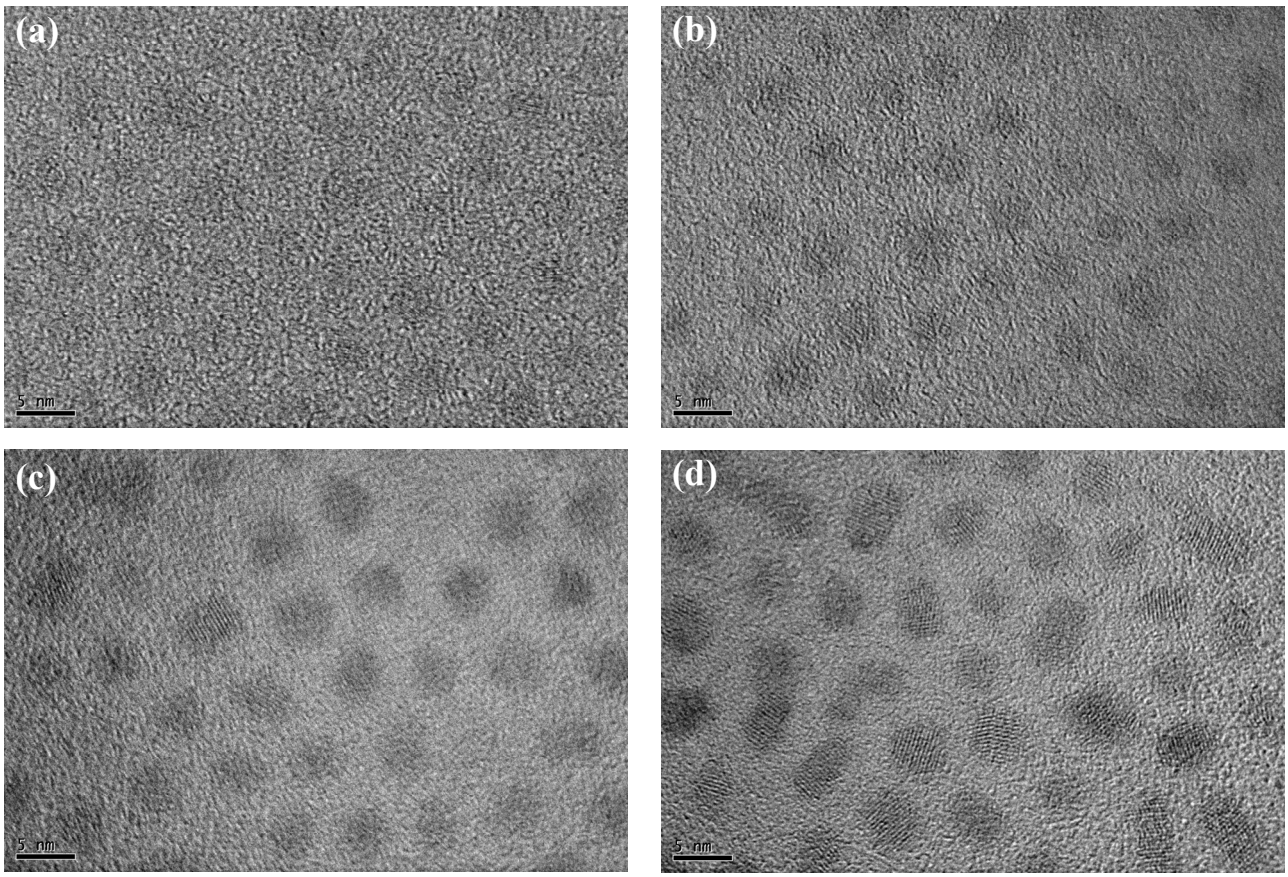

Fig. S4 HRTEM images of (a) Si QDs, (b) Si/CdS-1 NCs (c) Si/CdS-2 NCs and (d) CdS NCs. Scale bar: 5 nm.

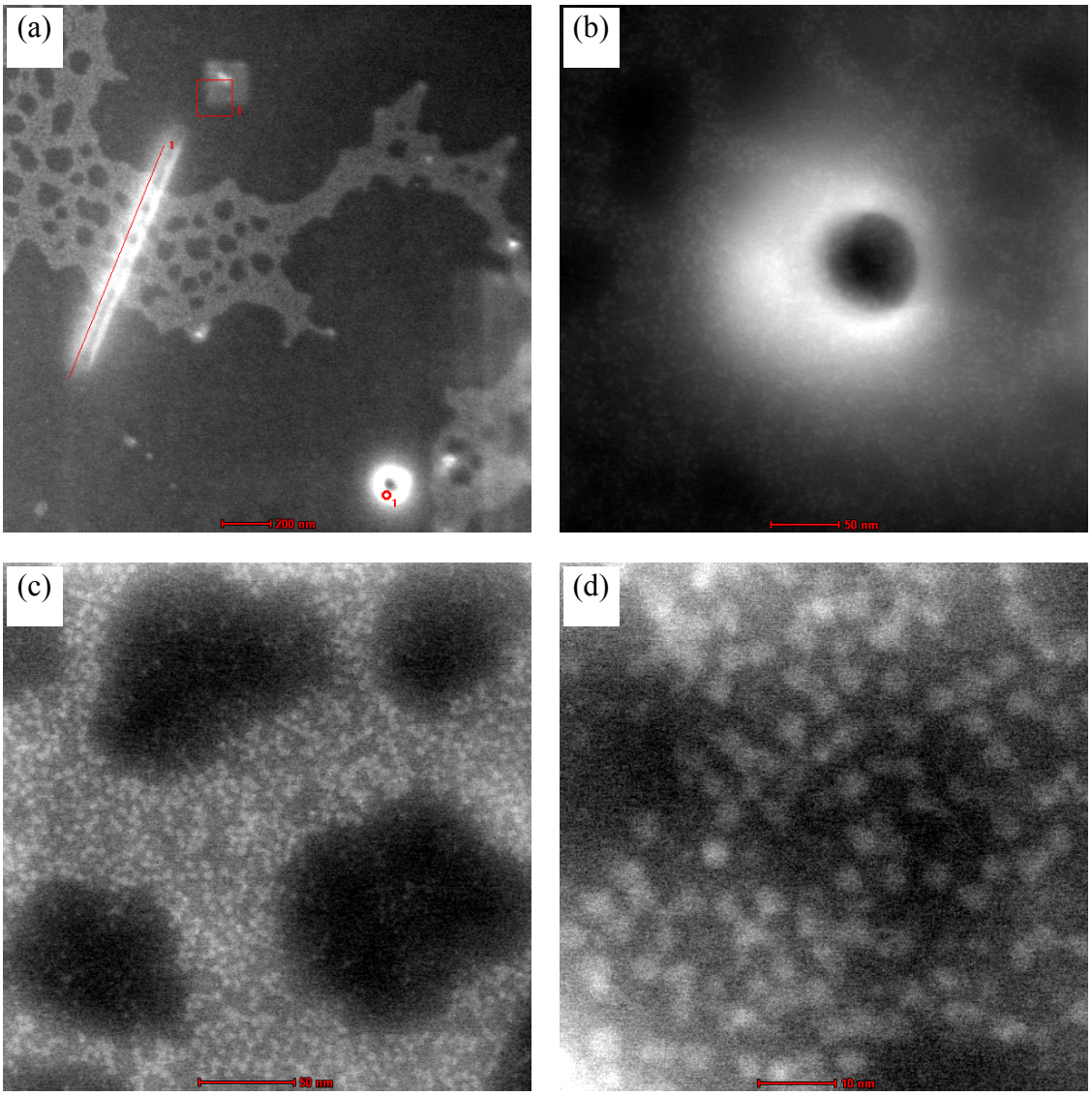

Fig. S5 (a) (b) When subjected to single or a few NCs EDS linear-scanning of the Si/CdS-2 NCs, the sample was suffered from damaging that possibly induced by degration/carbonization of the organic components. Area EDS spectrum show the existence of Si, Cd and S elements (Figure 1e). (c) (d) Scanning transmission electron microscope (STEM) images of the Si/CdS-2 NCs.

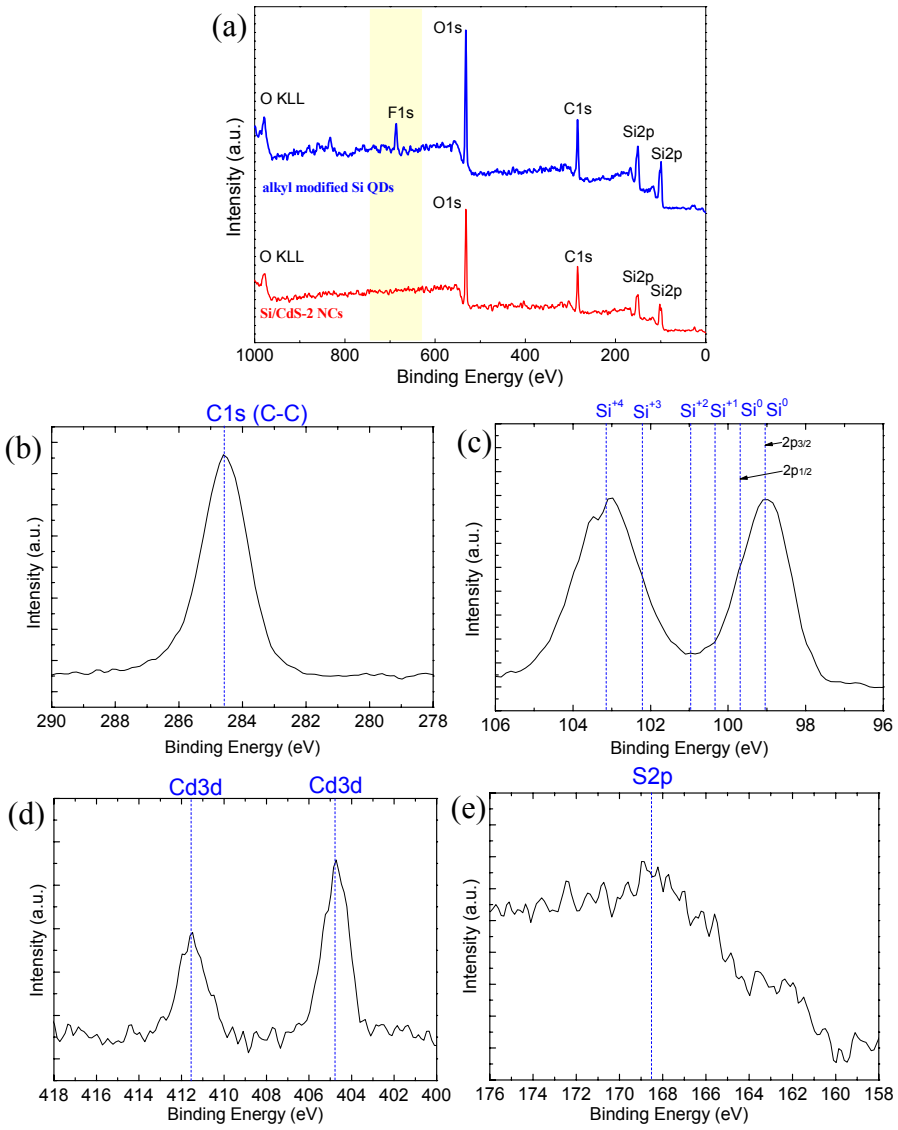

Fig. S6 (a) XPS survey spectra of Si/CdS-2 NCs and alkyl modified Si QDs. XPS spectra of (b) C1s, (c) Si2p, (d) Cd3d and (e) S2p of Si/CdS-2 NCs. The Si QDs sample has an F1s peak at 686 eV. The fluoride, possibly in the form of Si-F on the silicon surface, is induced by the HF etching procedure.[s1] The F1s is no longer detected in the XPS spectra of Si/CdS-1 and Si/CdS-2 NCs. Instead, Cd3d and S2p are observed by high-resolution XPS, suggesting the surface capping of CdS.

Derived by Brus using the effective mass approximation (EMA), when the nanocrystal radius is smaller than Bohr radius, the effective band-gap energy $E_{g,eff}$ is given by:[s2]

$$E_{g,eff} = E_g + \frac{\hbar^2 \pi^2}{2\mu R^2} - \frac{1.8e^2}{4\pi\varepsilon_0 \varepsilon R} + smaller\ terms \quad (1)$$

where E_g is the bulk band-gap energy, R is the nanocrystal radius, $\hbar$ is Planck's constant divided by 2π, μ is the effective reduced mass, and ε is the effective dielectric coefficient. Approximately,

$$E_{g,eff} = E_g + \Delta E_e + \Delta E_h, \text{ where } \Delta E_e = \frac{\hbar^2 \pi^2}{2R^2} \cdot \frac{1}{m_e^*},\ \Delta E_h = \frac{\hbar^2 \pi^2}{2R^2} \cdot \frac{1}{m_h^*} \quad (2)$$

m_e^* and m_h^* are the effective masses of electron and hole, respectively. In a first approximation, $m_e^* \approx 2m_h^*$ for Si and $m_h^* \approx 4m_e^*$ for CdS, it predicts that for Si QDs the valence band should shift twice the shift of the conductance band; and for CdS nanoparticles the conductance band should shift fourth the shift of the valence band for the bandgap widening contribution. The effective band-gap energy $E_{g,eff}$ of Si QDs and CdS NCs shown in Figure 2e is deduced from the band edge emission peak of the photoluminescence spectrum, and the band position is calculated by equation (2) above.

Table S2 Fitting parameters of the PL decay curves and PL quantum yield (QY).

Sample	Emission (nm)	τ_1 (ns)	τ_2 (ns)	τ_3 (ns)	a_1	a_2	a_3	R-Square	τ_{av} (ns)	QY (%)
CdS NCs	474	1.3	9.8	85.9	0.68	0.19	0.13	0.984	70.2	1.5
	683	76.9	433.3	1741.1	0.53	0.46	0.1	0.997	949.7	
Si/CdS-1	430	1.2	1.2	7.8	0.48	0.47	0.05	0.997	3.1	4.0
	560	6.1	41.9	161.5	0.51	0.35	0.14	0.999	104.7	
Si/CdS-2	467	1.4	5.6	75.1	0.72	0.28	0.003	0.999	9.5	2.4
	675	8.8	79.4	436.9	0.59	0.31	0.1	0.999	288.6	
Si QDs	630	5.30E4	1.02E5	-	0.47	0.53	-	0.999	86625	1.7

Note: $a_i = \frac{A_i}{\sum_{j=1}^{n} A_j}$, i=1,2,3, n=3 for CdS, Si/CdS-1 and Si/CdS-2 NCs; i=1,2, n=2 for Si QDs.

The PL decay curves are fitted to the exponential function:

$$I(t) = \sum_{i=1}^{n} A_i \exp(-(t - t_0)/\tau_i) \quad (3)$$

Where τ_i is the PL decay lifetime; A_i is the weighting parameter; n=3 for CdS and Si/CdS samples; n=2 for Si QDs. The fitting parameters are given in **Table 1**. The average lifetimes are determined by the equation:[s3]

$$\tau_{av} = (\sum_{i=1}^{n} A_i \tau_i^2) / (\sum_{i=1}^{n} A_i \tau_i) \quad (4)$$

The quantum yields (QY) of the samples were measured with coumarin 540 dye in methanol as a reference (91%).[s4] The low QY of CdS and Si/CdS NCs (1–4%) may be due to the relatively low reaction temperature of 180–200 °C and 1:1 of the Cd to S precursor ratio used.[s5] The mild temperature is favored for the control of the SILAR growth of shell, suppressing independent CdS nucleation and preventing the oxidization of Si QDs; meanwhile, it degenerates crystallinity, resulting high defect density, thus inducing lowered QY and prominent surface states (or defect states) photoluminescence. The stoichiometric ratio of the precursors is a prerequisite for the SILAR growth of shell and prohibits independent nucleation, but at the same time it leads to lower QY than using excess of one of the precursors.[s5] The balance of these parameters is required for the optimization of the structure and QY of the Si/CdS NCs. Despite the low QY, the QY of Si/CdS-2 is of 60% higher than that of the CdS NCs sample. This increased QY possibly results from the defects in the CdS shell being less than in CdS NCs, for the relative intensity of the surface state emission to the band edge emission is lower for the Si/CdS-2 sample than for the CdS NCs (Figure 2b). Another possibility could be the trapping of the holes in the CdS shell. The trapping of holes may result a quasi 'reverse type-I' structure of the Si/CdS NCs. This is supported by the facts that the PL from CdS shell is not quenched because of the proposed charge separation but even enhanced compared with the CdS NCs, and that in type-I core/shell NCs the PL decay lifetime can be shortened compared with the core.[s6]

s1. X. Cheng, S. B. Lowe, P. J. Reece, J. J. Gooding. *Chem Soc Rev*. **2014**, 43, 2680.

s2. L. E. Brus, *J. Chem. Phys.* **1984**, 80, 4403.

s3. a) T. Fujii, K. Kodaira, O. Kawauchi, N. Tanaka, *J. Phys. Chem. B*, **1997**, 101, 10631; b) B. K. Gupta, T. N. Narayanan, S. A. Vithayathil, Y. Lee, S. Koshy, A. L. Reddy, A. Saha, V. Shanker, V. N. Singh, B. A. Kaipparettu, A. A. Martí, P. M. Ajayan, *Small*, **2012**, 8, 3028.

s4. J. N. Ritty, K. J. Thomas, V. K. Jayasree, C. P. Girijavallabhan, V. P. N. Nampoori, P. Radhakrishnan, *Appl. Optics*, **2007**, 46, 4786.

s5. a) L. Wang, J. Wang, Y. Chen, H. H. Zhong, Y. Jiang, *Chem. J. Chin. Univ*., **2011**, 32, 1043; b) L. H. Qu, X. G. Peng, *J. Am. Chem. Soc*., **2002**, 124, 2049.

s6. a) M. A. Hines, P. Guyot-Sionnest, *J. Phys. Chem.*, **1996**, 100, 468; b) D. S. Liang, L. Shen, Z. B. Wang, Y. P. Cui, J. Yu. Zhang, Y. H. Ye, *Chin. Phys. Lett*., **2008**, 25, 4431.